Egyptian Journal of Chemistry

http://ejchem.journals.ekb.eg/

Kinetics of pyrolysis of water hyacinth: A novel empirical approach

Y.A. AbdelRaouf[1], H. M. AbdelHady[1], M.F. Abadir[1], H.A. Sibak[1]

[1]The Chemical Engineering Department, Faculty of Engineering, Cairo University

Abstract

An empirical method based on the equation of the sigmoid shape of the conversion –temperature curve was applied on the pyrolysis of water hyacinth to produce biochar. The dried material was manually ground to pass 147μm screen and its calorific value determined. The material was heated in nitrogen in a thermal analyzer at four different heating rates (5 to 20°C.min⁻¹). The TG trace obtained was used to calculate the conversion to biochar which was completed at about 400°C with subsequent cracking up to about 500°C. The produced biochar was characterized by EDX and its calorific value determined. Equations were obtained for the sigmoid shapes to simulate the conversion – temperature curves at the four heating rates. A simple method was then used to predict the kinetic parameters of biochar formation and cracking relying on the sigmoid shapes of conversion curves. These were found to be compatible with that calculated by the Coats – Redfern method.

Key words: Biochar – Hyacinth – Kinetics – Sigmoid

1. Introduction

The kinetics of combustion and pyrolysis of different types of biomass has been the subject of a large number of publications. Most authors agreed that pyrolysis takes place on steps associated with the loss of physical water and devotilization of organic volatile fractions (cellulose, hemicellulose and lignin). At the end of these steps, biochar is formed. Numerous authors have investigated the kinetics of pyrolysis of various types of biomass often obtaining disparate values of activation energy for the stages of decomposition of the same biomass when using different kinetic models in their calculations [1 – 6]. A comprehensive review of the models used in assessing the different kinetic parameters in the pyrolysis of biomass was given by Nunes et al [7]. They reviewed the different kinetic models and concluded that there could be large differences in values of activation energy on applying different techniques or on varying the rate of heating.

The first attempt to investigate the decomposition kinetics of water hyacinth was carried out by Luo et al [8] who found out that the main decomposition step took place in the stage of degradation corresponding to the devolatilization of cellulose and hemicellulose. They used the Coats – Redfern method assuming a first order reaction to evaluate the activation energy of that step and obtained a value of 116kJ.mol⁻¹. Sukarni et al [9] also studied thermal decomposition behavior of water hyacinth in nitrogen flow. They obtained a global value of activation energy of 60.74 kJ/mol. On the other hand, Wauton et.al [10] prepared bio-oil from the pyrolysis of water hyacinth in a fixed bed reactor. The pyrolysis was carried out at 450°C in a nitrogen stream. They reported a figure of 34.18 kJ.mol⁻¹ for the activation energy of formation of biochar. Also, Gulab et al [11] studied the catalytic pyrolysis of water hyacinth using waste Cu and Al as catalysts and obtained a maximum bio-oil yield of 31.6%. Bora et al [12] carried out pyrolysis in nitrogen flow of hyacinth and obtained three distinct regions for its degradation. An average activation energy of 238.75kJ.mol⁻¹ on the conversion range 0.1 – 0.8 was obtained. On the other hand, Phiwchaaum et al [13], on researching the kinetics of degradation of hyacinth and polystyrene obtained a range of values for activation

_____

energy of devolatilization of the organic portions from 67.6 to 132.8 kJ.mol^{-1}, depending on the assumed model of reaction. Much higher values for activation energy were obtained by Muigai et al using four non – model methods for kinetic analysis, the figures obtained varying from 187.7 to 329.71 kJ.mol^{-1} [14]. The effect of co-pyrolysis of water hyacinth with coal was investigated by Sukarni et al [15] who found out that the global activation energy decreased from 84.02kJ.mol^{-1} for pure coal to 44.45kJ.mol^{-1} for pure hyacinth. On the other hand, Liu et al [16] found out that biochar from biomass particles was generally generated at about 400°C and ended cracking at about 530°C. More recently, Liu et al [17] used Aspen plus software to simulate successfully the pyrolysis of biomass and disclose the mechanism of biochar formation.

In the present paper, a novel kinetic model was elaborated to predict the kinetic parameters of the reactions associated with the pyrolysis of water hyacinth, these parameters being of major importance in the design of pyrolysis reactors. This model takes advantage of the sigmoid shape of the conversion – temperature curves common to most solid state decomposition reactions.

2. Experimental

Hyacinth samples were washed three times using tap water, then sun dried for three days. The dried samples were washed with distilled water then dried in electrical oven at 100°C for one hour to then ground in a rotary cutter. They were then screened to pass 100 mesh screen (147μm).

About 10mg of dried specimens of the waste were placed in a thermal analyzer of type TGA-50H – Shimadzu type that could be operated at heating rates ranging from 2 to 50°C.min^{-1}. TGA and DTG data could be retrieved as both spreadsheets and curves.
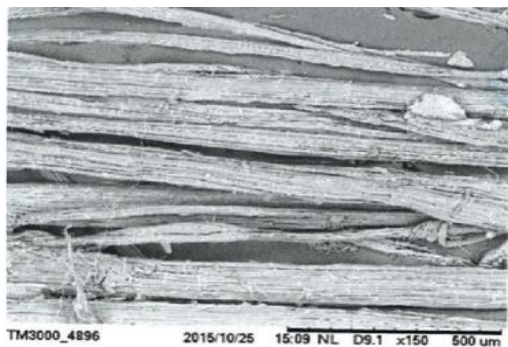

Fig 1: Hyacinth fibers (150×) [18]

_____

The heating rates used were 5, 10, 15 and 20°C.min^{-1} in nitrogen at flowing at the rate of 50mL.min^{-1}.

FTIR was used to determine the functional groups constituting hyacinth. The infrared spectra of samples were measured using Class1 Laser Product IEC/EN 60825-1/A2:2001 Avatar Series.

The calorific value of dry water hyacinth was determined using Parr 6200 bomb calorimeter.

EDX characterization of biochar, prior and after cracking, was carried out using an INTERTEK type analyzer.

3. Results and discussion
3.1 Physical appearance of dried hyacinth sample
Dry hyacinth possesses a fibrous nature as can be observed from the micrograph (150×) reported by Chonsakom et al [18] shown in Fig 1.
3.1 FTIR Characterization of water hyacinth
Fig 2 illustrates the FTIR pattern of water hyacinth whereby the functional groups corresponding to wave numbers at IR peaks were interpreted as revealed in Table 1
3.2 Determination of calorific value
The calorific value of dried water hyacinth was determined using a bomb calorimeter. The net calorific value was found to equal 13600 kJ.kg^{-1}, a value slightly less than that obtained by Larra-Serrano et al (14400kJ.kg^{-1}) [20]. Compared to other types of biomass, the determined calorific value for dried water hyacinth seems reasonable enough to consider its use as biofuel. It compares fairly with the values obtained for other vegetable waste as evidenced from Table 2.

3.3 TG – DTG curves for hyacinth decomposition
The TG – DTG curves obtained displayed the presence of three distinct peaks, neglecting the small peak observed below 100°C corresponding to loss of moisture. Following the work of several authors, such as Wang et al [26] and Xiao et al [27], the step resulting in the formation of biochar involves the devolatilization of hemicellulose, cellulose and lignin. Fig 3 shows the TG – DTG traces obtained at a heating rate of 5°C.min-1. The results obtained at higher rates were similar except that the peak temperatures were shifted to higher values.

The first main DTG peak observed corresponds to the previously mentioned devolatilization ending at about 400°C, a figure frequently quoted for the temperature

of formation of biochar [12, 28]. The second peak relates to cracking of biochar starting at about 420ºC and ending at 620ºC. These temperatures increase by increasing the heating rate. A third small peak corresponding to a slight loss in weight (3.2%) corresponds to combustion of the remaining char owing to the presence of about 1.8% oxygen with the flowing nitrogen stream as indicated in Fig3.

Fig 4A displays the EDX analysis of the biochar retrieved after heating to 400ºC, while Fig 3B shows the analysis of the same specimen when heated to 520ºC. Cracking has had for effect to eliminate gaseous hydrocarbons, thus reducing the carbon content from 49.87% to 18.97%. Also, volatile

components containing nitrogen seem to have completely disappeared as evidenced by the lack of nitrogen element in Fig 4B.

The main region of interest in the present work is that corresponding to the formation of biochar, corresponding to the first major DTG peak. Table 3 displays the temperature at which that step starts, that of the observed peak and the final temperature at which the step ends, at all four investigated heating rates.
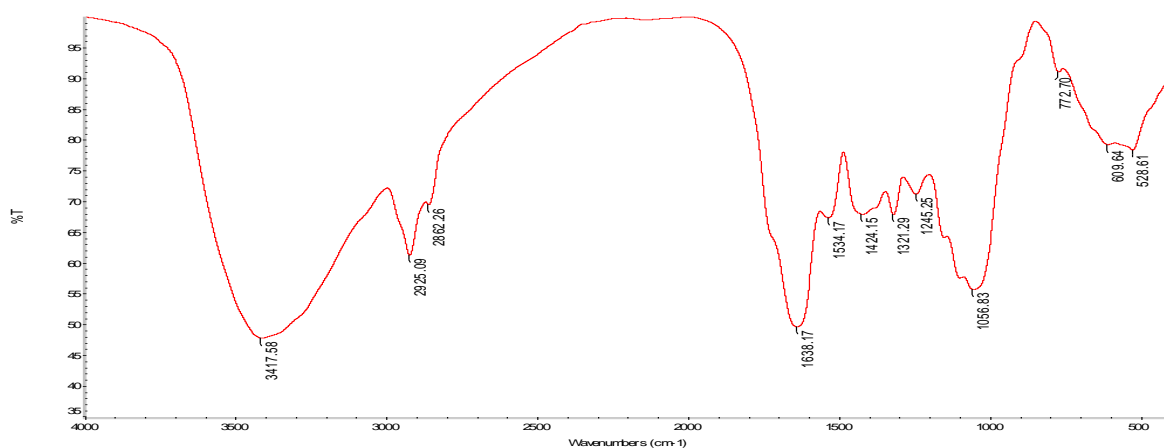

Fig 2: FTIR pattern of dry water hyacinth

Table 1: Functional groups of water hyacinth [19]

Wave number cm^{-1}	Band origin
3417.58	O-H stretch, alcohols
2925.09	C-H vibration; alkane
2862.23	CH-CH$_2$ stretch
1435.21	C-H vibration; alkane
1638.17	C=O stretch, carboxylate; KBr
1534.17	C=C Aromatic skeletal vibration of lignin C=N ; C-N amides
1424.17	C-H deformation asymmetric
1321.29	C-H deformation asymmetric
1056.83	C-O Stretch

Table 2: Net calorific value of some vegetable waste (kJ.kg^{-1})

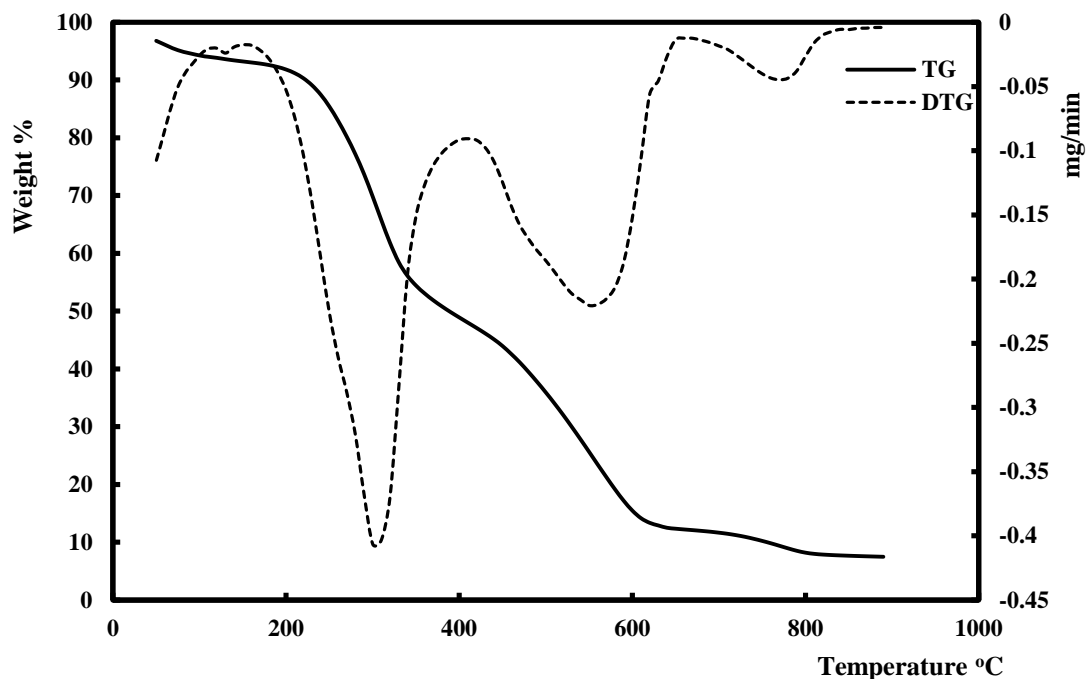| Waste	Banana peels	Orange peels	Rice straw	Rice husk	Wheat straw
Cal. Value	14800	12630	13900	13400	14640
Reference	21	22	23	24	25

Fig 3: TG – DTG curves for the pyrolysis of hyacinth at 5°C.min⁻¹

Table (3): Characteristic temperatures for the first decomposition step of water hyacinth

Rate of heating β °C.min⁻¹	5	10	15	20
T_i °C	160	170.1	180.2	192
T_p °C	303.4	314.1	323	328.2
T_f °C	400	409.4	425.9	437.5

The calorific value of the biochar formed at 400°C was determined using a bomb calorimeter. The value obtained = 17200kJ.kg⁻¹, a value compatible with that obtained by Munjeri et al (14000 to 20000kJ.kg⁻¹) [29]

3.4 Conversion curves for the first step of decomposition of water hyacinth

From the spreadsheets obtained from the thermal analyzer, it was possible to calculate the conversion at any temperature along a TG step form the definition:
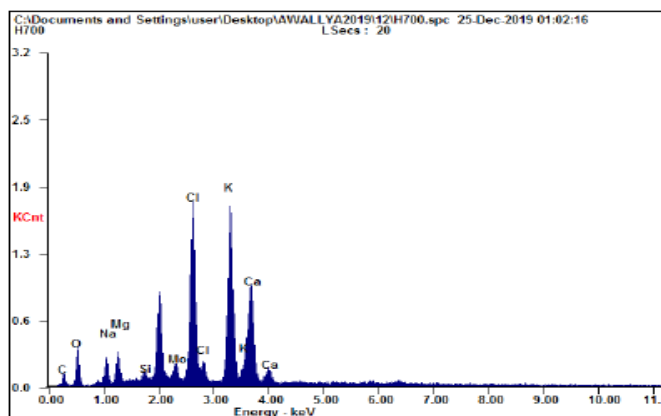
Element	Wt %	At %
C K	18.97	34.03
O K	23.22	31.28
NaK	04.77	04.47
MgK	03.72	03.30
SiK	01.16	00.89
MoL	03.61	00.81
ClK	14.52	08.83
K K	18.29	10.08
CaK	11.75	06.32

Fig 4A: EDX Analysis for the biochar obtained from hyacint
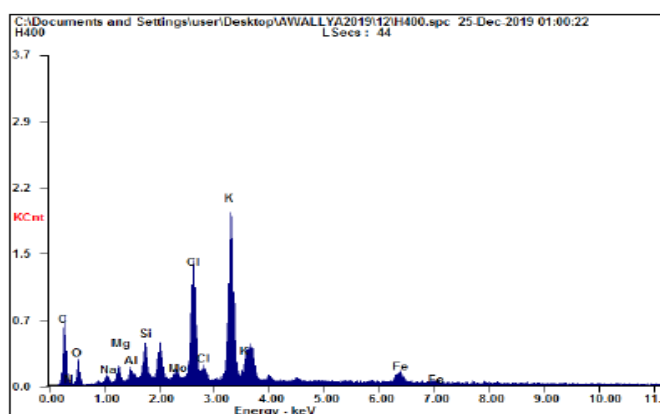
Element	Wt %	At %
C K	49.87	67.01
N K	05.24	06.04
O K	12.53	12.64
NaK	01.32	00.93
MgK	01.49	00.99
AlK	01.11	00.66
SiK	02.45	01.41
MoL	01.75	00.29
ClK	07.81	03.55
K K	13.98	05.77
FeK	02.45	00.71

Fig 4B: EDX analysis for cracked biochar from hyacinth

$$\alpha = \frac{m_0 - m}{m_0 - m_f} \tag{1}$$

Where, m_0 and m_f are the initial and final masses respectively

Fig 5 illustrates the conversion – temperature curves at the different heating rates.
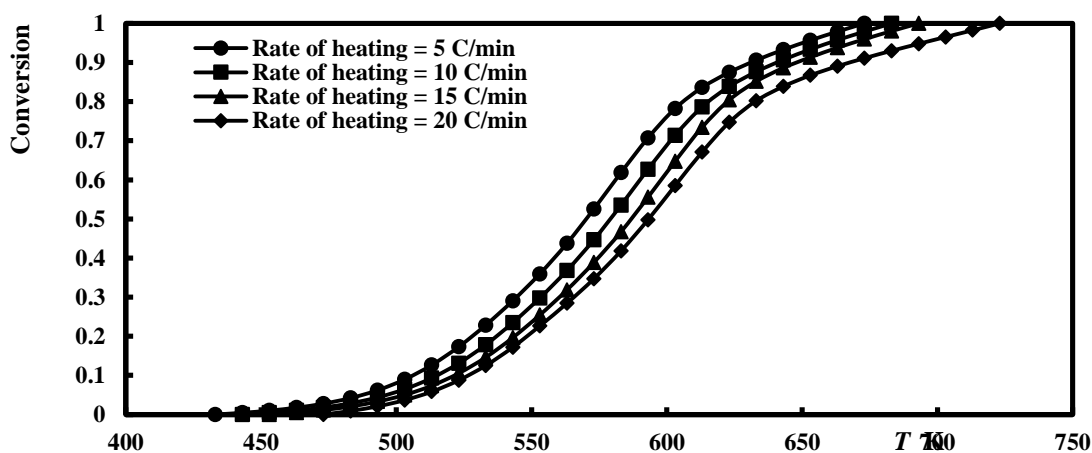

Fig 5: Conversion – Temperature curves for hyacinth (Step 1)

3.5 Elaboration of a model

As observed from that figure, all four curves take sigmoid shapes. The equation of the general sigmoid curve takes the form [30]:

$$\alpha = f(t) = \frac{1}{1 + e^{-(a+bT)}} \tag{2}$$

Where, L, a and b are constants and T, the temperature (K)

Rearranging, one gets:

$$\ln\frac{1-\alpha}{\alpha} = -(a + bT) \tag{3}$$

This means that a plot of the LHS against temperature should result in a straight line of slope — b and intercept — a

Such plots have been carried out for all four rates and the resulting almost parallel straight lines obtained displayed in Fig 6. This assesses the validity of working out calculations based on a sigmoid function.

Next, the activation energy was determined using the following procedure: The rate of reaction is proportional to $\frac{d\alpha}{dt}$ and its expression can be deduced by differentiating equation (2). The obtained derivative can then be recombined with equation (2) to yield:

$$\frac{d\alpha}{dT} = b\alpha(1 - \alpha) \tag{4}$$

The rate of heating $= \beta = \frac{dT}{dt}$ (5)

$$\frac{d\alpha}{dt} = \frac{d\alpha}{dT} \cdot \frac{dT}{dt} = \frac{d\alpha}{dT} \cdot \beta = b\beta\alpha(1 - \alpha) \tag{6}$$ The generalized model free kinetic equation takes the form [31]

_____

$$\frac{d\alpha}{dt} = Ae^{-\frac{E}{RT}}.f(\alpha) \qquad (7)$$

For an apparent order of reaction n, the previous equation reads:

$$\frac{d\alpha}{dt} = Ae^{-\frac{E}{RT}}.k.(1-\alpha)^n \qquad (8)$$

Where, k is the reaction rate constant.

Equating equations (6) and (8) we get:

$$b\beta\alpha = k.Ae^{-\frac{E}{RT}}.(1-\alpha)^{n-1} \qquad (9)$$

Although most authors assume that biochar is formed through a first order reaction ($n = 1$) [7, 10], it was thought more appropriate to rewrite the previous equation in the more general form:

$$b\beta\alpha(1-\alpha)^{1-n} = k.Ae^{-\frac{E}{RT}} \qquad (10)$$

$$\ln\alpha\,(1-\alpha)^{1-n} = \ln k.A - \ln b\beta - \frac{E}{RT} \qquad (11)$$

Hence a plot of $\ln\alpha\,(1-\alpha)^{1-n}$ against $1/T$ should result in a straight line of slope $= -\frac{E}{R}$

Values of n were chosen and the value corresponding to a maximum determination coefficient (R^2) between the values of $\ln\alpha\,(1-\alpha)^{1-n}$ and $\frac{1}{T}$ were obtained at each heating rate (using the "solver" function available on EXCEL). The apparent order of reaction n was found to equal 0.46 (Corresponding to a minimum value of $R^2 = 0.997$). The plots of $\ln\alpha\,(1-\alpha)^{0.54}$ against $\frac{1}{T}$ are shown in Fig 7 and reveal the presence of almost parallel straight lines.

The following table lists the values of activation energies (E) calculated at each heating rate from the slopes of the lines from which an average activation energy was calculated to equal 72.22kJ.mol^{-1}. The values of activation energy obtained at different heating rates are fairly close to the activatin energy for the whole decomposition process reported by Sukarni et al [9].

3.6 Results obtained using the Coats – Redfern method (First step)

To check the validity of the suggested method, the Coats – Redfern method was applied on the present data.

The basic kinetic equation in that method takes the following form [32]:

$$\ln\frac{g(\alpha)}{T^2} = -\frac{E}{RT} + \ln\frac{A.R}{E.\beta}.\left(1 - \frac{2R.T_{av}}{E}\right) \qquad (12)$$

Where, $g(\alpha)$ is chosen from the table of integral kinetic functions according to the prevailing mechanism. Khawam et al [31] have summarized the different mechanisms associated with solid – gas reactions in Table 5.

An expression for $g(\alpha) = k.t$ is chosen from that table and a plot performed between $\ln\frac{g(\alpha)}{T^2}$ and $1/T$ for different heating rates. The slope obtained is then used to calculate the activation energy.

This method was applied on the present data for conversion and the plots illustrated in Fig 8. The highest value of R^2 was obtained on assuming that decomposition takes place at the surface of the solid. This corresponds to the following form for $g(\alpha)$ corresponding to surface reaction for cylindrical shapes.

This checks with the fibrous nature of ground hyacinth particles (Fig 1) [19].

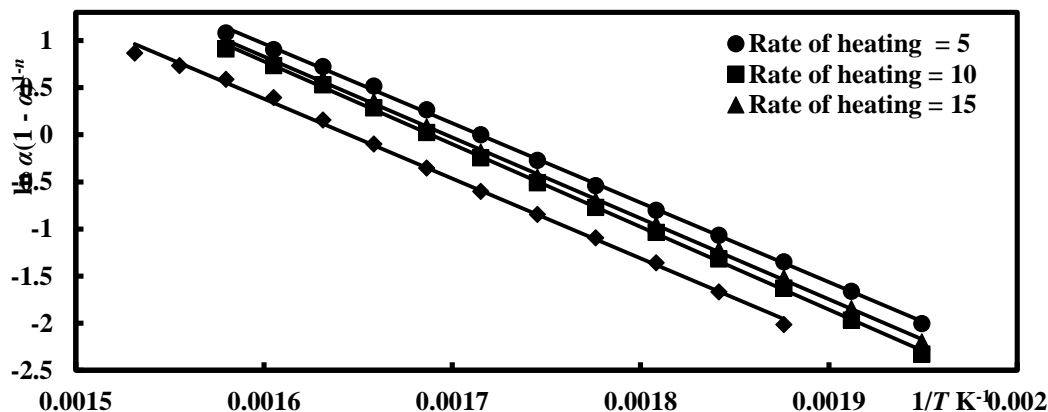$$g(\alpha) = kt = 1 - (1-\alpha)^{\frac{1}{2}} \qquad (13)$$

Fig 6: Linearized curves for Conversion – Temperature for hyacinth (First step)
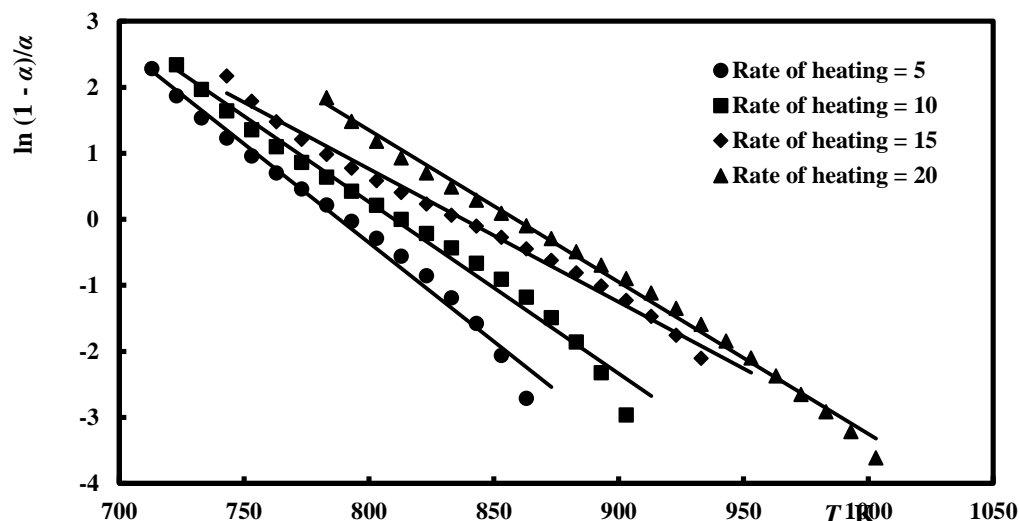
_____

Fig 7: Curves for the suggested model as applied to hyacinth decomposition (First step)

Table (4): Values of activation energy for biochar formation using the sigmoid model

Heating rate β °C.min^{-1}	5	10	15	20
E kJ.mol^{-1}	69.73	72.52	74.35	72.27
R^2	0.999	0.997	0.999	0.998

Table (5): Different forms of the kinetic function $g(\alpha) = k.t$ [31]

Controlling step	$g(\alpha) = k.t$
Avrami-Erofeev	$[-\ln(1-\alpha)]^{1/m}$
First order model	$-\ln(1-\alpha)$
nth order reaction ($n \neq 1$)	$\dfrac{(1-\alpha)^{1-n}}{1-n}$
Spherical: reaction at interface	$1-(1-\alpha)^{\frac{1}{3}}$
Spherical: diffusion through ash	$1-\dfrac{2}{3}\alpha-(1-\alpha)^{\frac{2}{3}}$
Spherical: diffusion through gaseous layer	A
Cylindrical: reaction at interface	$1-(1-\alpha)^{\frac{1}{2}}$
Cylindrical: diffusion through ash	$\alpha+(1-\alpha).\ln(1-\alpha)$
Spherical: shrinking coarse particles	$1-(1-\alpha)^{\frac{1}{2}}$
Spherical: shrinking fine particles	$1-(1-\alpha)^{\frac{2}{3}}$

The following table gives the values of activation energy obtained at each rate. They yield an average activation energy of 66.19kJ.mol^{-1}, a value fairly close to that obtained by the present model (72.22kJ.mol^{-1}) and by Sukarni et al [9] but definitely not as high as that obtained by Luo et al [8] (116 kJ.mol^{-1}) or Bora et al [12] (284 kJ.mol^{-1})

One point of interest is that the differentiation of equation (13) yields an expression for the rate of reaction in the form:

$$\frac{d\alpha}{dt} = k.(1-\alpha)^{\frac{1}{2}} \qquad (14)$$

The apparent order of reaction hence equals 0.5, a value almost identical to that obtained using the present model (0.46).

3.7 Conversion curves for the second step of decomposition of water hyacinth

As previously stated, this step relates to the cracking of biochar. The conversion – temperature curves and the linearized plots of $\ln\frac{1-\alpha}{\alpha}$ against $1/T$ for the second step of decomposition of water hyacinth are shown in Fig 9. Table 7 illustrates the variation of the initial, peak and final temperatures for that step.

3.8 Application of the suggested model on the kinetics of cracking of biochar

On applying the suggested model, the best fit value of the exponent n in equation 11 at all heating rates, corresponding to a minimum value of $R^2 = 0.978$,

was $n = 1.2$. The plots of $\ln\alpha\,(1-\alpha)^{1-n}$ against $\frac{1}{T}$ are illustrated in Fig 10. The values of activation energy as calculated from the slopes at the four heating rates are reported in Table 8. This table shows fairly close values of E with an average value of 62.31kJ.mol^{-1}, a value almost twice that obtained by Wauton et.al (34.18) [10] but much lower than that obtained by Muigai et al (187.7 to 329.71 kJ.mol^{-1}) [14]. The large discrepancies in activation energy and the fact that its value can vary with heating rate have been recently detailed by Altanzis et al [33] on researching the kinetics of pyrolysis of peach seeds and subsequent cracking of biochar. Also, close values of activation energy ranging from 60 to 65 kJ.mol^{-1} were obtained by Saeed et al [34] on investigating the fast pyrolysis of jatropha seeds.

Table (6): Activation energy for biochar formation (Coats – Redfern method)

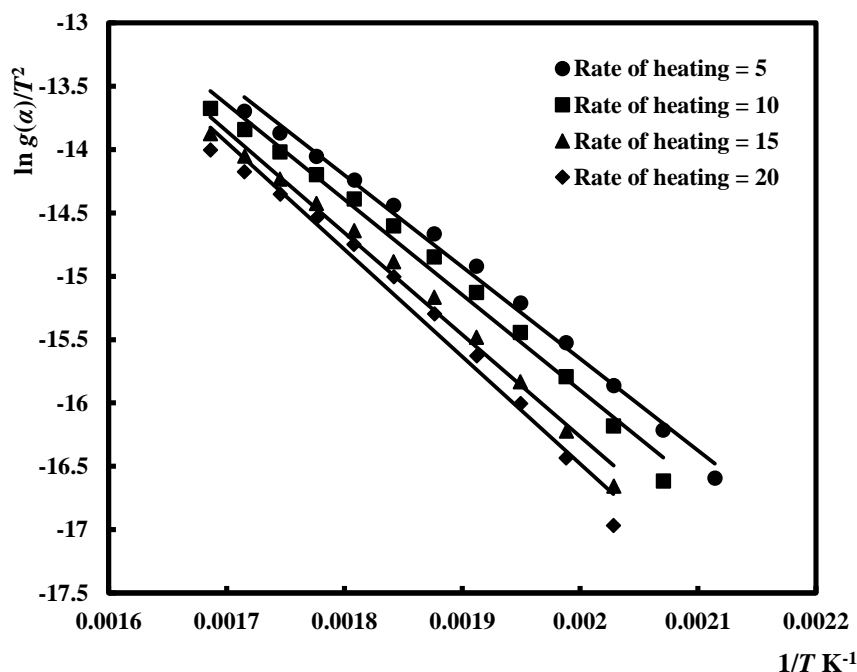| β °C.min^{-1}	5	10	15	20
E kJ.mol^{-1}	59.02	66.62	68.82	70.29

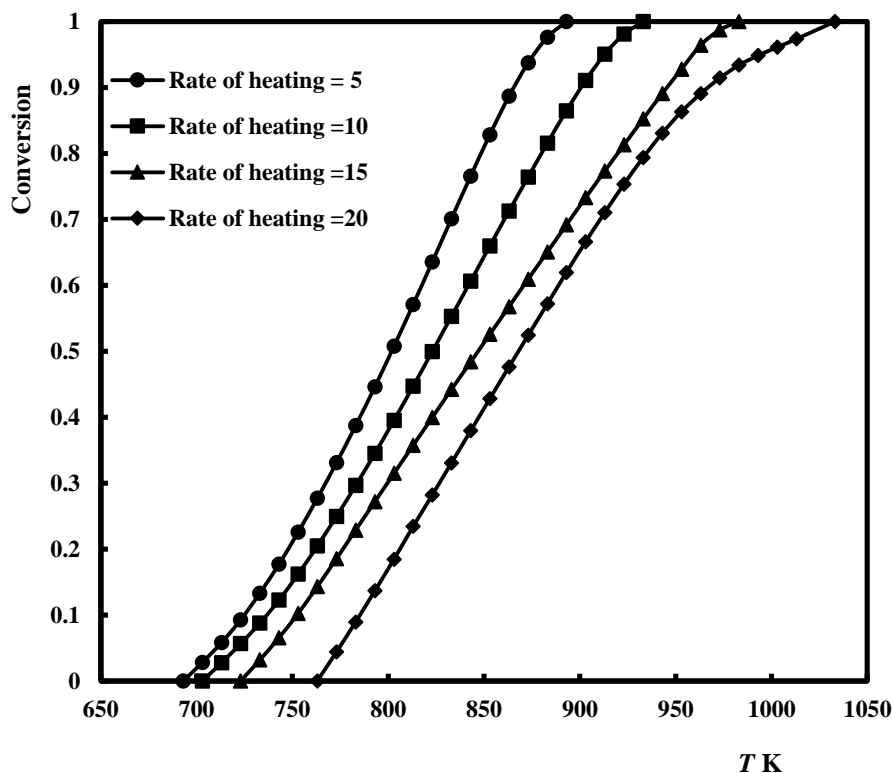Fig 8: Coats – Redfern plots for the formation of biochar

Fig 9: Conversion – Temperature curves for hyacinth (Step 2)

Table (7): Characteristic temperatures for the first decomposition step of water hyacinth

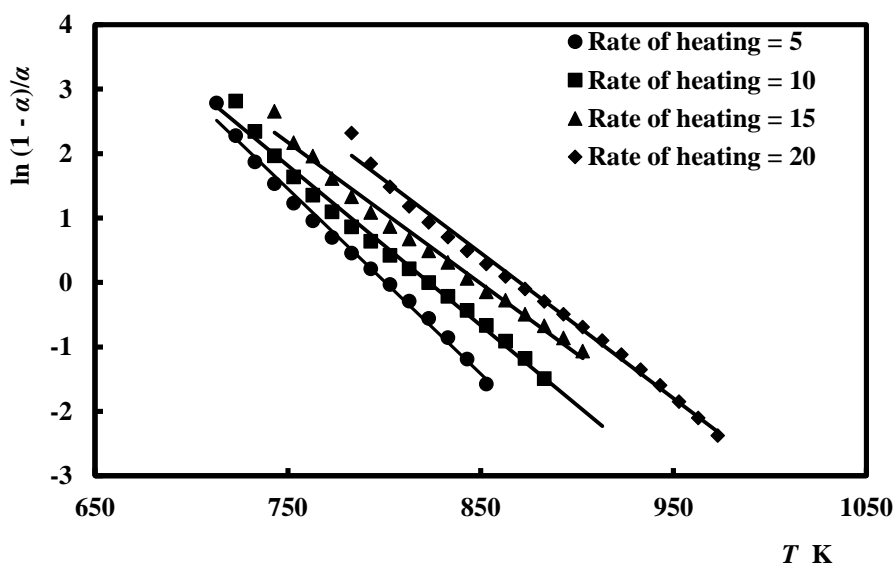| Rate of heating β ºC.min⁻¹	5	10	15	20
T_i ºC	420	429.9	450.3	488.5
T_p ºC	554.2	571.4	582	593
T_f ºC	622	660	708	760

Fig 10: Linearized curves for Conversion – Temperature for hyacinth (Step 2)

_____

Table (8): Activation energy for cracking of biochar (Sigmoid model)

β °C.min^{-1}	5	10	15	20
E kJ.mol^{-1}	69.3	66.35	54.5	59.11

3.9 Results obtained using the Coats – Redfern method (Second step)

The application of the Coats – Redfern method to determine the kinetic parameters for that step requires assuming a certain form for the conversion function $g(\alpha)$ to be chosen from Table 4. Since the sigmoid model has resulted in an apparent order of reaction = 1.2, it was reasonable to assume first order kinetics for that step following the expression:

$$g(\alpha) = kt = -\ln(1-\alpha) \qquad (15)$$

When values of $\ln \frac{g(\alpha)}{T^2}$ were plotted against $1/T$ for different heating rates, straight lines were obtained (Fig 12). The values of R^2 obtained ranged from 0.988 to 0.998, which validates the first order assumption. The activation energy at each heating rate was determined from the slopes of these lines and their values are reported in Table 9. The average activation energy = 62.02, kJ.mol^{-1}, a value almost identical to that obtained using the suggested sigmoid model (62.31).

4. Conclusions

Pyrolysis of dried water hyacinth was carried out in nitrogen atmosphere at heating rates ranging from 5°C.min^{-1} to 20°C.min^{-1}. TG – DTG curves showed the presence of two main weight losses corresponding to devolatilization of cellulosic material and cracking of the formed biochar. The functional groups present in hyacinth were determined using FTIR and a calorific value of 13600 kJ.kg^{-1} was obtained using a bomb calorimeter. Also, EDX imaging was used to determine the elemental analysis of the char obtained and its cracking residue. The carbon content of the formed char at about 400°C $\approx$ 50% (By weight) decreasing to about 19% at 520°C due to cracking. The calorific value of the formed biochar was determined to equal 17200kJ.kg^{-1}.

A novel technique was suggested to investigate the kinetics of decomposition that relies on the sigmoid shape of conversion curves. The apparent order of reaction and average activation energy were determined accordingly and compared to the corresponding values obtained on applying the Coats – Redfern technique. The two methods yielded close results as revealed from the following table.
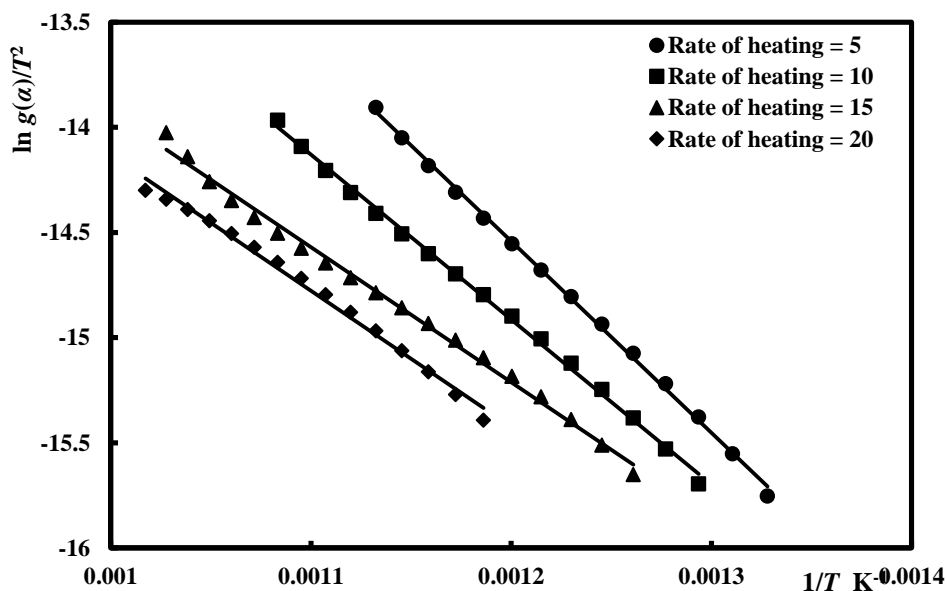

Fig 11: Curves for the sigmoid model as applied to cracking of biochar

_____

Table (9): Activation energy for cracking of biochar (Coats-Redfern model)

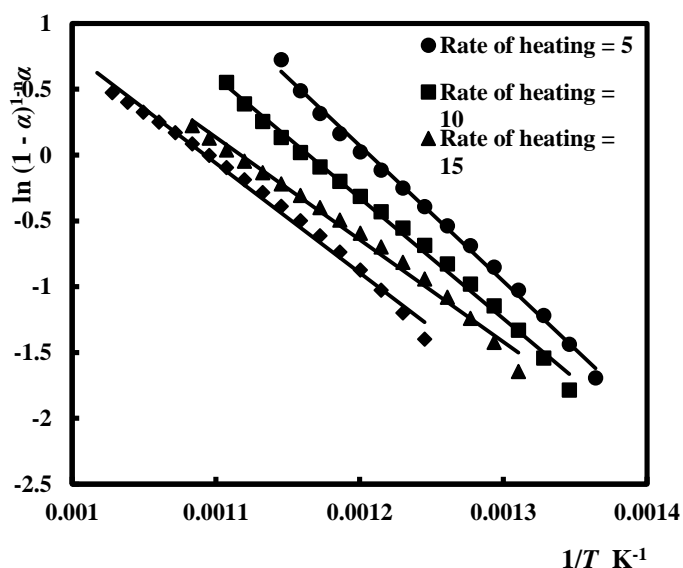| β °C.min^{-1}	5	10	15	20
E kJ.mol^{-1}	75.70	65.18	53.38	53.73

Fig 12: Coats – Redfern plots for cracking of biochar

Table (10): Comparison between kinetic parameters obtained by the suggested method and Coats – Redfern method

Method	Step	Sigmoid	C – R
Activation energy, kJ.mol^{-1}	First step	72.22	66.19
	Second step	62.31	62.02
App. Order of reaction, n	First step	0.46	0.5
	Second step	1.2	1

REFERENCES

1- A.Y. Liang, S.N. Hui and T.M. XuTG-DTG "Analysis and combustion kinetics characteristic study on several kinds of biomass". *Renewable Energy Research* vol. 26, pp. 56-61 (2008).

2- Y. Qiguo, F. Qi, G.D. Chang, Y. Zhang, B. Xiao, Z. Hu, S. Liu, H. Kai and S. Xu "Thermogravimetric analysis of co-combustion of biomass and biochar" *Journal of Thermal Analysis and Calorimetry* Vol. 112, issue 3, pp. 1475-1479 (2013)

3- Q. Wang, W. Zhao, H. Liu, C. Jia and H. Xu "Reactivity and Kinetic Analysis of Biomas during Combustion" *Energy Procedia* Vol. 17(A), pp. 869-875, (2012)

4- A. Alvarez, C. Pizarro, R. Garcia and J.L. Bueno "Determination of kinetic parameters for biomass combustion" *Bioresearch Technology*, Vol. 216, pp. 36-43 (2016)

5- M.V. Kok and E. Özgür "Thermal analysis and kinetics of biomass samples" *Fuel Process Technology*, Vol. 106, pp. 739-743 (2013)

6- L.B. dos Santos, M/V/ Striebeck, M. Crespi, J.M.V. Capela, C. Ribeiro and M. De Julio "Energy evaluation of biochar obtained from the pyrolysis of pine pellets" *Journal of Thermal Analysis and Calorimetry* Vol. 126, issue 3, pp. 1879-1887 (2016)

_____

7- L.J.R. Nunes, J.C.O. Matias, and J.P.S. Catalão, "Mixed biomass pellets for thermal energy production: A review of combustion models," *Applied Energy*, vol. 127, pp. 135–140 (2014)

8- G. Luo, J. Strong, H. Wang, W. Ni and W. Shi "Kinetics of the pyrolytic and hydrothermal decomposition of water hyacinth" *Bioresearch Technology* Vol. 102, issue 13, pp. 6990 – 6994 (2011)

9- S. Sukarni, A. E. Widiono, S. Sumarli, R. Wulandari, I. M. Nauri and a. A. Ayu, "Thermal decomposition behavior of water hyacinth (eichhornia crassipes) under an inert atmosphere," MATEC *Web of Conferences*, vol. 204, (2018)

10- I. Wauton and S. E. Ogbeide, "Characterization of pyrolytic bio-oil from water hyacinth (Eichhornia crassipes) pyrolysis in a fixed bed reactor" *Biofuels*, Vol. 12, Article no 8 (2021)

11- H. Gulab, K. Hussain, S. Malik and a. M. Hussain, "Effect of Process Conditions on Bio-oil Composition and Production from Catalytic Pyrolysis of Water Hyacinth Biomass," *Waste Biomass Valorization*, Vol. 10, pp. 2595-2609 (2019)

12- B.J. Bora, D. Mallick, S.A. Barbhuiya and R. Banik "Pyrolysis kinetics of water hyacinth using thermogravimetric analysis" International Conference on Advanced Materials for Energy Science and Technology (AMEST) (2019)

13- C. Phiwchaaum, B. Ksapabutr, N. Chaiyutand and M. Panapoy "Kinetic study for the co-pyrolysis of water hyacinth biomass with waste polystyrene" *Material Science and Engineering*, Vol. 965, Article no 012029 (2020)

14- H.H. Muigai, B.J. Choundhury, P. Kalita and V. Moholkar "Physico–chemical characterization and pyrolysis kinetics of *Eichhornia Crassipes, Thevetia Peruviana,* and *Saccharum Officinarum*" *Fuel*, vol. 289, Article no 119949, (2021)

15- S.Sukarni, N.Mufti, A.A.Permanasari, R.E. Ardianto and A. Johari "The fitting kinetic evaluation during co-pyrolysis of coal and water hyacinth (Eichhornia crassipes) to explore its potential for energy" AIP Conference Proceedings 2255, 030035 (2020)

16- L.Liu, Y.Pang, Lv D., K.Wang and Y. Wang "Thermal and kinetic analyzing of pyrolysis and combustion of self-heating biomass particles" *Process safety and Environment Protection.* Vol. 151, pp. 39-50 (2021)

17- Y.Liu, X.Yang, Zhang J. and Z. Zhu "Process simulation of preparing biochar by biomass pyrolysis via Aspen plus and its economic evaluation" *Waste Biomass Valorization* (2022). https://doi.org/10.1007/s12649-021-01671-z

18- S. Chonsakom, S. Srivorradatpaisan and R. Mongkholrattanasit "Effects of different extraction methods on some properties of water hyacinth fibers" *Journal of Natural Fibers*, vol. 16, issue 7, pp. 1-11 (2018)

19- IR Spectrum Tables and Charts: https://www.sigmaaldrich.com/EG/en/technical-documents/technical-article/analytical-chemistry/photometry-and-reflectometry/ir-spectrum-table

20- J.S. Larra-Serrano, O.M. Rutiaga-Quiñones, J. López-Miranda, H.A. Fileto-Pérez, F.E. Pedraza-Bucio, J.L. Rico-Cerda and J.G. Rutiaga-Quiñones "Physicochemical characterization of water hyacinth (Eichhornia crassipes)" Bioresearch, vol. 11, issue 3, pp.7214-7223 (2016)

21- I. Kabenge, J. Umilo, N. Bannada, J. Seay, A. Zziwa, N. Kiggundu "Characterization of banana peels wastes as potential slow pyrolysis feedstock" *Journal of Sustainable Development* vol. 11, issue 2, pp. 14-24 (2018)

22- B. Velàsquez-Marti, I. López-Cortés, D. Salazar-Hernández, A.J. Callejón-Ferre "Modeling the calorific value of biomass from fruit trees using elemental analysis data" Book Chapter in: Biomass volume estimation and Valorization for energy, DOI: 10.5772/65276 (2017)

23- N. Van Hung, M. C. M-Detras, M. V. Migo, R. Quilloy, C. Balingbing, P. Chivenge, M. Gummert "Rice straw overview" Book Chapter in: Sustainable rice straw management, pp. 1-13, Springer, Cham. https://doi.org/10.1007/978-3-030-32373-8_1

_____

24- H, Sadig, H.A. Suleiman, M. N. Zaidi-Moni, L. D. Anbealagan "Characterization of date palm frond as a fuel for thermal conversion processes" *MATEC Web of Conferences* 131, 01002 (2017)

25- GG. Bradna, J, Malatak, D. Hájek "The properties of wheat straw combustion and use of fly ash as a soil amendment" *Agronomy Research*, vol. 14, issue 4, pp. 1257-1265 (2016)

26- S. Wang, G. Dai, H. Yang, and Z. Luo "Lignocellulosic biomass pyrolysis mechanism: A state-of-the-art review" *Progress in Energy and Combustion Science* vol. 62, pp. 33-86 (2017)

27- R. Xiao, W. Yang, X. Cong, K. Dong, J. Xu, D. Wang and X. Yang, X "Thermogravimetric analysis and reaction kinetics of lignocellulosic biomass pyrolysis" *Energy*, Vol. 201: Article no 117537 (2020)

28- L. Luo, X. Guo, Z. Zhang, M, Chai, M.M. Rahman, X. Zhang and J. Cai "Insight into pyrolysis kinetics of lignocellulosic biomass: Isoconversional kinetic analysis by the modified Friedman method" *Energy Fuels* vol. 34, issue 4, pp. 4874-4881 (2020)

29- K. Munjeri, S. Ziuku, H. Maganga, B. Siachingoma and S. Ndlovu "On the potential of water hyacinth as a biomass briquette for heating applications" *International Journal of energy and Environmental Engineering* Vol. 7, issue 1, 10.1007/s40095-015-0195-8 (2015)

30- A. Kocian, G. Carmassi, F. Cela, L. Incrocci, P. Milazzo and S. Chessa "Bayesian Sigmoid-Type Time Series Forecasting with Missing Data for Greenhouse Crops" *Sensors* (Basel) Vol. 20, issue 11, Article no 3246 (2020)

31- A. Khawam and D.R Flanagan "Solid state kinetic models: Basics and mathematical fundamentals," *Journal of Physical Chemistry* B, vol. 110, issue 35, pp. 17315-17328 (2006)

32- E. Urbanovici, C. Popesku and E. Segal "Improved iterative version of the Coats-Redfern method to evaluate non-isothermal kinetic parameters," *Journal of Thermal Analysis and Calorimetry*, vol. 58, pp. 683-700 (1999)

33- A-I Altanzis, N-C. Kallistridis, G. Stavropoulos and A. Zabaniotou "Apparent pyrolysis kinetics and index-based assessment of pretreated peach seeds" *Processes*, vol. 9, Article no 905 (2021)

34- Sh. Saeed, I. Ashour, H. Sherif and M.R.O. Ali "Catalytic and noncatalytic fast pyrolysis of jatropha seeds: experimental measurements and modeling" *Egyptian Journal of Chemistry*, Vol. 63, issue 2, pp. 383-702 (2020)

كيناتيكا الإنحلال الحراري لورد النيل: نموذج وضعي مبتكر

تم تطبيق نموذج وضعي يعتمد علي شكل المنحني السيجمويد الذى يربط بين نسبة التحويل و درجة الحرارة في عملية الإنحلال الحرارى لنبات ورد النيل بغرض دراسة كيناتيكا التحول إلي الفحم الحيوي. تم طحن النبات المجفف ليمر من منخل فتحة 147 ميكرون و تم تعيين قيمته الحرارية. تم التسخين في جو من النيتروجين بمعدلات تسخين تتراوح من 5 إلي 20 ˚م/دقيقة. أوضح منحني التغير الوزني أن التحلل إلي الفحم الحيوي يكتمل عند حوالي 400 ˚م ثم يحدث تكسير لهذا الفحم ينتهي عند حوالي 500 ˚م. تم توصيف الفحم الحيوي قبل و بعد التكسير باستخدام و تم تعيين القيمة الحرارية له. تم استنتاج معادلات لمحاكاة شكل منحنيات التحول و تم ابتكار نموذج بسيط للتنبؤ بالثوابت الكيناتيكية لعملية تكون الفحم الحيوي و تكسيره. تم مقارنة النتائج التي تم الحصول عليها من خلال النموذج المقترح بطريقة كوتس – ردفيرن و ظهر تطابقا جيدا بين الطريقتين.